Set membership estimation applied to the localization of small UAS in tight flight formations

J Bolting, Soheib Fergani

Set membership estimation applied to the localization of small UAS in tight flight formations

J. Bolting[1], S. Fergani[2*]

***Abstract*— This paper proposes a set membership approach for UAS (unmanned aerial system)localization in a tight flight formation. A novel set membership estimation strategy based on the typical hardware available for localization (due to the cost constraints put on small UAS for civil applications) is developed. The main idea is as follows: using time-differenced differential GNSS carrier phase observations, the relative position between UAS can be tracked with centimeter-level precision, but affected by an unknown constant meter-level bias due to the initial coarse position standalone position estimate. Using pseudorange observations, as well as UWB range observations, the guaranteed space containing this position bias is determined using dense box particle sampling and sequential purging. The carrier phase trajectory fully captures the dynamics of the UAS motion and enables precise relative position holding from t = 0 on. The proposed set membership filter scheme is fully complementary to and independent of any other algorithm employed to estimate the relative position.**
simulation results of the problem of cooperative relative localization between UAS on a formation flight benchmark compared to a standard Extended Kalman Filter illustrate the benefits arising from the deterministic nature of set membership filtering. .

I. Introduction

In the recent years, the proliferation of small unmanned aircraft systems (UAS) for military applications has also led to new expansion of the use of the unmanned vehicle in several civilian domains and markets. According to a new report of the World Civil Unmanned Aerial Systems Market Profile & Forecast by the Teal Group, the market for civil, commercial and consumer drones will expand from 2.8 billion in 2017 to an annual level of more than 11.8 billion by 2026 a compound growth rate of 15.5 percent.
Recently, a lot of studies have tried to provide pertinent solution for the control and localization of the uas especially in tight formation flight (see [1]).
Tight formation flight is an enabling technology for a large number of range enhancing techniques such as upwash exploitation, aerial recharging and aerial docking between UAS. The corresponding major technological challenges lie in reliably and accurately maintaining relative position in the wake of another aircraft, while guaranteeing collision avoidance. Indeed, Localization errors generally have a greater detrimental effect on formations of small UAS than larger ones, since admissible guidance errors scale with airframe size. A lot of strategies have provided solutions for this problem. Indeed, COTS consumer grade GNSS hardware provides relative localization errors in the centimeter range are possible using readily available RTK (Real-Time-Kinematics) algorithms,(see e.g. [2]). Also, Alternative GNSS-independent approaches such as machine vision have been considered but generally provide less accuracy, among other reasons owing to attitude estimation errors of low-cost AHRS (Atitude Head Reference System), affecting the critical transformation of observations in the camera frame to the local inertial frame, see e.g. ([3]).
In this work, set membership localization algorithm is proposed to give safety guarantees when it comes to relative positioning between aircraft. Here, the developed set membership filtering scheme provides both guaranteed regions and point estimates of the relative position between UAS. The proposed strategy uses time-differenced differential GNSS carrier phase observations, the relative position between UAS can be tracked with centimeter-level precision , but affected by an unknown constant meter-level bias due to the initial coarse position standalone position estimate. Using pseudorange observations, as well as UWB range observations, the guaranteed space containing this position bias is determined using dense box particle sampling and sequential purging. The carrier phase trajectory fully captures the dynamics of the UAS motion and enables precise relative position holding from t = 0 on. It can be employed in a complementary fashion parallel to possible existing point localization algorithms such as the Extended Kalman Filter or in a complete independent way of any other algorithm employed to estimate the relative position. The resulting bounds could also be used to detect divergence of other estimation schemes such as the EKF or to define a guaranteed search region for GNSS ambiguity resolution. The proposed scheme shares the advantage of other set membership algorithms that it does not require assumptions on the statistical distribution of measurement errors, but only an interval within which they can be guaranteed to reside, obtainable from long-term static measurements. Also, this algorithm can readily be applied to manned aircraft, where safety guarantees are key to making commercial manned tight formation flight a reality in the future.

The paper is organized as follow: in Section 1, problem statmement is presented. Then, in Section 2 the set membership estimation strategy is proved. In Section 3, simulations performed on a formation flight benchmark compared to a

[1] ISAE-SUPAERO, Conception and control of aerospatial vehicles DCAS department, ISAE- SUPAERO - 10 avenue Edouar Belin, Toulouse - Cedex FRANCE
[2]* LAAS-CNRS, Decision and Optimization DO department,7, avenue du Colonel Roche BP 54200 31031 Toulouse cedex 4, France. Corresponding author: soheib.fergani@laas.fr

standard Extended Kalman Filter prove the efficiency of the proposed solution. Finally, in Section 4. Conclusions and future works are presented in the last section.

Remark 1: In this work, GNSS relative position tracking and Differential carrier phase localization are used but will no be detailed (due to paper length restrictions).

II. Problem statement

To take into account error of relative position estimates, not only point estimates of relative position vectors are required, but rather an outer estimate of the regions that can be guaranteed to contain the other members of the formation. We want furthermore this estimate to be useful, i.e. only as large as necessary and relying only on sensors realistically available on board a typical small low cost UAS. What is more, the employed algorithm needs to be compatible with the still somewhat limited computational resources of todayś small UAS.

A. Assumptions and constraints

Hardware resources We assume that in view of cost and mass constraints weighing in particular on small UAS for civil applications, the set of observations and state estimates available for localization is limited to: The image stream of a single camera, fixed in the body frame. Attitude estimates and observations of angular rates, accelerations and the earthś magnetic field in the body frame provided by a MEMS based AHRS. Single-frequency GNSS carrier phase, Doppler and pseudo range observations. UltraWide Band (UWB) inter-UAS ranging observations. In the following, a modified Extended Set Membership Filter (ESMF) compatible with the assumed limited set sensor hardware is presented.

III. Set membership localization

Existing localization approaches rely mostly on RTK (Real-Time-Kinematics) GNSS (Global Navigation Satellite System) positioning, machine vision or a combination of both (in [4]). The standard approach of GNSS RTK systems provides, after ambiguity resolution, estimates of the position vector between two GNSS receivers with the millimeter-level accuracy of carrier phase positioning. The drawbacks of this approach lies within flight safety conditions. First, before ambiguities are fixed, only probabilistic bounds on the estimation error of the float solution are available. Second, once ambiguities are fixed, a small nonzero probability that the fixed set of ambiguities is not the actual one remains, due to the statistical nature of the fixing algorithm. For this sake, new strategies to enhance differential GNSS localization both on the pseudo range level and for RTK solutions have been developed, as the very cost effective Ultra Wide Band (UWB) ranging modules based on time of flight observations. Then, the machine vision which approaches suffer from the fundamental limitation that tracked UASs need to be within the field of view of the tracking UAS for each filter update, necessitating multiple of gimballed cameras in larger formations as well as trajectory planning algorithms that take into account maintaining continuous visual contact.

Also, both technics have been employed in the community for accurate relative localization of UAS and centimeter level precision is reported in experimental settings, again employing an Extended Kalman Filter. Even if it can indeed provide an ellipsoidal confidence set that is guaranteed to contain the true state with a selected probability given that its underlying assumptions of normally distributed, zero mean modeling errors and measurement errors are met, as is well known, in reality both error sources can only be approximated by it and filter consistency needs to be ensured by careful tuning. What is more, Kalman filters, being based on probabilistic error models, provide estimates of stochastic state estimation error bounds. Even given a consistent estimate, probabilistic bounds can however only guarantee probabilistic collision avoidance.

Since Guaranteed bounds of estimation errors are however of crucial importance for flight safety. here, we present a Modified Extended Set membership filtering that is concerned with the problem of providing tight estimates of these bounds.

A. notations and definitions

1) Interval notations and definitions: In this work, we use a general interval matrix notation $[x]$ for the family of matrices $x \in \mathbb{R}^{n\times m}$ where $x_{i,j} \in [\underline{x}_{i,j}, \overline{x}_{i,j}]$, for $i = 1....n$,$j = 1..,m$. For $n > 1, m = 1$, $[x]$ is an interval column vector, for $n = 1, m = 1$, $[x]$ is an interval scalar.
though, for additive errors used in the paper, the following enter-range notation for intervals is used as $[x] = x + [wx]$ where x is the center point of $[x]$ and $[wx] = [x] - \frac{1}{2}[x; x]$ where $[x; x]$ denotes a degenerate interval containing only the point x. all operations in the expression are interval operations.

2) Interval extensions: Interval extensions of various basic operators and functions ($+, -\frac{1}{2}$, exp, log etc.) are known to be sharp inclusions of the real result sets. When constructing interval extensions of more complex functions, care needs to be taken, as alternative but equivalent formulations of the same function can lead to different, possibly heavily conservative result intervals. This fundamental issue appears when a variable appears more than once in an expression. In this paper,as a useful exception, for (piecewise) monotonic functions dependency issues can be circumvented altogether (in [5]).

3) Ellipsoids - Definitions and Notations: The proposed ESMF strategy relies on ellipsoidal set approximations. An ellipsoid in $\mathbb{R}$ is given by

$$\Omega(x_c, P) = \{x|(x - x_c)^T P^{-1}(x - x_c) \leq 1\} \qquad (1)$$

with $x \in \mathbb{R}^n$ some point in space, $x_c \in \mathbb{R}^n$ the ellipsoid center and a positive definite matrix $P \in \mathbb{R}^{n\times m}$ defining half axes and orientation.
An alternative representation employed for ellipsoid intersections with a strip (used in this work) is as follow:

$$E_c(x_c, V) = \{x|x = xc + Vw, \|w\| \leq 1\} \qquad (2)$$

Useful for analyzing ellipsoid size metrics and displaying the ellipsoid surface in 3 dimensions. Note that equation (1) can be decomposed into a diagonal matrix $P_0 \in \mathbb{R}^{n\times n}$ (corresponding to an axes-aligned ellipsoid) carrying the squares of the half axes on its diagonal and a matrix $R^{n\times n}$ performing the rotation to its original attitude

$$(x - x_c)^T(\mathbf{R}^T P_0 \mathbf{R})^{-1}(x - x_c) \leq 1 \tag{3}$$

The columns of $\mathbf{R}$ are the eigenvectors of P^{-1}, while the diagonal of P_0 can be computed from the eigenvalues of P^{-1}. For $n = 3$, $\mathbf{R}$ is the DCM (Direction Cosine Matrix) defined by the half axis unit vectors of the ellipsoid forming a right-handed Cartesian frame (see [6]).

B. Modified Extended Set Membership Filter

In the spirit of the Extended Kalman Filter, the Extended Set Membership Filter proposed ([7]) extends ellipsoidal set membership filtering to nonlinear systems by local linearization. Ellipsoidal bounds on the resulting linearization errors are employed and lumped together with the propagation error bounds and measurement error bounds of the nonlinear model. The algorithm is rather generic as the propagation and update step provide sets of approximating ellipsoids, each parametrized by a scalar parameter. While mentioning the existence of closed form minimum trace solutions, it proposes applying numerical optimization to determine the parameter corresponding to the minimum volume ellipsoid in each set. Note that the utilization of numerical optimization does not preclude real-time application, since every member of the given sets is guaranteed to contain the propagated set or intersection respectively, so optimization can be stopped anytime. Closed-form solutions are however preferable due to improved efficiency (especially taking into account the still somewhat limited embedded computing resources of UAS) and guaranteed minimization of the selected size criterion. Then, in ([8]) the minimum trace solution can directly be applied to the propagation step. On the other hand, no minimum trace or minimum volume closed form exist solutions for the update step in its form given by ([7]).
In the following we present a modified, fixed time version of the ESMF, adopting the closed form minimum trace ellipsoid approximations proposed in ([8]). First **the algorithm** in general terms is provided, followed by specifics for **relative UAS localization**.

Remark 2: For the proposed ESMF, we consider in a first step GNSS (Global Navigation Satellite System) code phase and carrier phase observations. We then integrate UWB (Ultra Wide Bande) ranging observations as a first step to robustify the localization scheme and investigate how this additional information affects filter performance. In the following GNSS and inter-UAS ranging observation models and their respective linearizations are required. For sake of brevity and due to the article size limitations, Authors will not present all the details that can be found in literature.

The algorithm extends ellipsoidal set membership filtering to nonlinear systems by local linearization. The general idea is to first propagating the guaranteed state set $\Omega(\hat{x}_{k,k}, \Sigma_{k,k})$ of the preceding filter step k propagated using the dynamics model and an ellipsoidal bound $\Omega(0, Q_k)$ modeling error. This amounts to forming the Minkowski sum of $\Omega(\hat{x}_{k,k}, \Sigma_{k,k})$ and $\Omega(0, Q_k)$. This sum generally not being an ellipsoid, an outer ellipsoidal approximation $\Omega(\hat{x}_{k+1,k}, \Sigma_{k+1,k})$ is formed minimizing some measure of size. Then, the intersection of $\Omega(\hat{x}_{k+1,k}, \Sigma_{k+1,k})$ and an ellipsoidal approximation of the consistent state set is approximated by a bounding ellipsoid $\Omega(\hat{x}_{k+1,k+1}, \Sigma_{k+1,k+1})$ minimizing the trace of $\Sigma_{k+1,k+1}$ (this criterion leads to better behaved ellipsoids).

1) The algorithm: It is achieved using the following steps:

- **Propagation** We add an input term for state propagation by time differenced carrier phase observations

$$x_{k+1,k} = f(x_{k,k}) + u_k \tag{4}$$

where $x_k \in \mathbb{R}^n$ an unknown state contained the guaranteed set of the ellipsoid.

$$\Sigma_{k+1,k} = A_k \frac{\Sigma_{k+1,k}}{1 - \beta_k} A_k^T + \frac{Q_k}{\beta_k} \tag{5}$$

where $A = \frac{\partial f(x_k)}{\partial x}|_{x=\hat{x}_{k,k}}$ and compute the parameter β_k following [8] to minimize the trace of $\Sigma_{k+1,k}$

$$\beta_k = \left(\frac{tr(\Sigma_{k,k}^{1/2}(\Sigma_{k,k}^{1/2})^T)^{1/2} + tr(Q_{k,k}^{1/2}(Q_{k,k}^{1/2})^T)^{1/2}}{tr(Q_{k,k}^{1/2}(Q_{k,k}^{1/2})^T)^{1/2}} \right) \tag{6}$$

- **Update** The update step exploits the fact that a closed form minimum trace solution is possible for the intersection of ellipsoids and strips (more details about the closed form minimum trace [8]. Each element of the observation vector with its corresponding error interval defines a pair of hyperplanes - a strip - in state space, in turn defining the consistent space set as all states enclosed by the hyperplanes. By consecutive intersection of the propagated state ellipsoid with each strip, an approximation of the minimum trace ellipsoid intersection is obtained. From the linearized observation equation

$$\begin{bmatrix} y_{k+1,1} \\ \vdots \\ y_{k+1,m} \end{bmatrix} = \begin{bmatrix} C_1 \\ \vdots \\ C_m \end{bmatrix} x + \begin{bmatrix} \omega_{k+1,1} \\ \vdots \\ \omega_{k+1,m} \end{bmatrix} \tag{7}$$

where C_i are the rows of $C = \frac{\partial h(x_k)}{\partial x}|_{x=\hat{x}_{k,k}}$ and $\omega_{k+1,i} \in [-W_{k+1,i}, W_{k+1,i}]^3$ we obtain a set of m pairs of hyperplanes defining m strips in $\mathbb{R}^n$. The strips are recursively intersected with the propagated state ellipsoid $\Omega(\hat{x}_{k+1,k}, \Sigma_{k+1,k})$.
- **Recursive intersection**
Define

$$M = \Sigma_{k+1,k}^{-1} \tag{8}$$

$$c_0 = \hat{x}_{k+1,k} \tag{9}$$

For $i = 1, \ldots, m$
For each element of the observation vector the two

hyperplanes are given by

$$\begin{array}{rcl} \text{Plane 1}: & & \\ C_i||C_i||^{-1}x & = & (y_{k+1,i} - W_{k+1,i})||C_i||^{-1} \\ & = & p^+ \\ \text{Plane 2}: & & \\ C_i||C_i||^{-1}x & = & (y_{k+1,i} + W_{k+1,i})||C_i||^{-1} \\ & = & p^- \end{array} \tag{10}$$

with their common unit normal vector $C_i||C_i||^{-1}$ and the respective distances to the origin p^+, p^{-1}. As required by the intersection algorithm, we first check for each plane if it intersects the ellipsoid $\Omega(\hat{x}_{k+1,k}, \Sigma_{k+1,k})$, and if not, compute a parallel hyperplane that is tangent to the ellipsoid (see [9]). The resulting tightened hyperplanes being given by

$$\begin{array}{rcl} \text{Tightenedplane 1}: & & \\ C_i||C_i||^{-1}x & = & p_t^+ \\ & = & (y^{'}_{k+1,i} - \overline{W}_{k+1,i})||C_i||^{-1} \\ \text{Tightenedplane 2}: & & \\ C_i||C_i||^{-1}x & = & p_t^- \\ & = & (y^{'}_{k+1,i} + \overline{W}_{k+1,i})||C_i||^{-1} \end{array} \tag{11}$$

we compute a new tightened observation interval center

$$y^{'}_{k+1,i} = \tfrac{1}{2}(p_t^+ + p_t^-)||C_i|| \tag{12}$$

and tightened observation error bounds

$$\overline{W}_{k+1,i} = \tfrac{1}{2}(p_t^- - p_t^+)||C_i|| \tag{13}$$

The corresponding tightened strip has the same intersection with $\Omega(\hat{x}_{k+1,k}, \Sigma_{k+1,k})$ but simplifies the intersection algorithm, see ([8]). After normalizing with the new error bounds

$$\overline{y}_{k+1,i} = \overline{W}^{-1}_{k+1,i} y^{'}_{k+1,i} \tag{14}$$

$$\overline{C}_i = \overline{W}^{-1}_{k+1,i} C_i \tag{15}$$

we obtain a strip

$$S(\overline{y}_{k+1,i}, \overline{C}_i) = x : |\overline{y}_{k+1,i} - \overline{C}_i x| \leq 1 \tag{16}$$

in the form required for the intersection algorithm. The intersection of the ith strip and the intermediate ellipsoid $\Omega(c_{i-1}, M^{-1}_{i-1})$, is then computed as follows (adaption from [8]):

$$\begin{array}{rcl} P & = & M^{-1}_{i-1} \\ \delta & = & \overline{y}_{k+1,i} - \overline{C}_i c_{i-1} \\ g & = & \overline{C}_i P \overline{C}_i^T \\ \gamma & = & \overline{C}_i P^2 \overline{C}_i^T \\ \mu & = & tr(P) \\ \beta_1 & = & \frac{3}{g} \\ \beta_2 & = & \frac{g(\mu(1-\delta^2)-\gamma)+2(g\mu-\gamma(1-\delta^2))}{g^2(g\mu-\gamma)} \\ \beta_3 & = & \frac{\mu(1-detla^2)+\gamma}{g^2(g\mu-\gamma)} \end{array} \tag{17}$$

If $\beta_3 > 0$ the intersection does not modify $\Omega(c_{i-1}, M^{-1}_{i-1})$, i.e. both tightened hyperplanes are tangent and

$$\begin{array}{rcl} M_i & = & M^{-1}_{i-1} \\ c_i & = & c_{i-1} \end{array} \tag{18}$$

Otherwise the minimum trace ellipsoid bounding the intersection is computed as

$$\begin{array}{rcl} M & = & \frac{3\beta_2 - \beta_1^2}{9} \\ N & = & \frac{9\beta_1\beta_2 - 27\beta_3 - 2\beta_1^3}{54} \\ \theta & = & acos\left(\frac{N}{(-M^3)^{1/2}}\right) \\ q & = & 2(-M)^{1/2} cos\left(\frac{\theta}{3}\right) - \frac{\beta_1}{3} \\ \alpha^* & = & \frac{1}{1+q} \\ M_{\alpha^*} & = & \alpha^* M_{i-1} + (1-\alpha^*)\overline{C}_i \overline{C}_i^T \\ c_i & = & M^{-1}_{\alpha^*}[\alpha^* M_{i-1} c_{i-1} + (1-\alpha^*)\overline{C}_i \overline{y}_{k+1,i}] \\ \delta_{\alpha^*} & = & c^T_{i-1} M_{i-1} c_{i-1} + (1-\alpha^*)\overline{y}^2_{k+1,i} - c_i^T M_{\alpha^*} c_i \\ M_i & = & (1-\delta_{\alpha^*})^{-1} M_{\alpha^*} \end{array} \tag{19}$$

After the last intersection

$$\begin{array}{rcl} \hat{x}_{k+1,k+1} & = & c_m \\ \Sigma_{k+1,k+1} & = & M_m \end{array} \tag{20}$$

provide the updated guaranteed state ellipsoid at sample $k+1$.

2) Application to relative localization of UAS: We now apply the modified ESMF to the problem of cooperative relative localization between UAS. In a most basic configuration, each UAS runs a bank of filters, one for each other UAS. Computational effort could further be reduced by exchanging set estimates between UAS. In the following we consider the case of one UAS tracking the relative position of another one. To initialize the guaranteed state ellipsoid, the maximum error interval of the differential pseudo range position $\tilde{d}^{\rho,0}$ is computed by interval arithmetic from the least-squares solution of the GNSS code phase observations often denoted as pseudo ranges, of UAS i w.r.t. satellite p in units of distance (using the first order Taylor expansion and interval inclusion of linearization errors, more details in [7]).

$$[\tilde{d}^{\rho,0}] = (H_0^T H_0)^{-1} H_0^T [\nabla^r_{\rho_0}] \tag{21}$$

where $\nabla^r_{\rho_{p,i,j}}$ are the GNSS code phase observations differences between between two receivers on board UAS i and UAS j w.r.t. a reference satellite p. $H_{p,r} = \frac{\partial \nabla_{\rho_p}}{\partial d}|_{d=0}$ is the observation geometry matrix.

The Minimum Volume Ellipsoid (MVE) enclosing this interval provides then the initial guaranteed state set $\Omega(\hat{x}_{0,0}, \Sigma_{0,0})$.

The state comprises the relative position vector between UAS i and UAS j using the previously introduced algorithm

$$x_k = d_{i,j,k} \tag{22}$$

$$f(x_k) = d_{i,j,k} + \Delta\tilde{d}_k + w_{\Delta d,k+1} \tag{23}$$

$$A = I_3 \tag{24}$$

and observations are double differences of pseudo ranges

$$\begin{array}{rcl} y_k & = & \nabla^r_{\rho_k} \\ & = & H_{p,r} d_{i,j,k} + w_{\nabla^r_{p,k}} \\ C & = & H_{p,r} \end{array} \tag{25}$$

Note that we use the linearized observation equation here due to the small linearization error. The propagation error

ellipsoid $\Omega(0, Q_k)$ is obtained as the MVE of the interval of carrier phase position propagation errors $w_{\Delta_{d,k}}$ (from GNSS differential code phase observations.
To enhance the result of the UAS, we can use:

- **Incomporating the Ultra Wide Bande ranging**: Range observations are integrated into the filter by augmenting the observation vector to

$$\begin{aligned} y_k &= \begin{bmatrix} \nabla^r_{\rho_k} \\ r(i,j)_k \end{bmatrix} \\ &= \begin{bmatrix} H_{p,r} d_{i,j,k} + w_{\nabla^r_{p,k}} \\ ||d_{i,j,k}|| + \overline{w}_{r,k} \end{bmatrix} \end{aligned} \tag{26}$$

$$C = \begin{bmatrix} H_{p,r} \\ \frac{\partial r}{\partial d}|_{d=\hat{x}_{k,k-1}} \end{bmatrix} \tag{27}$$

  where r is the relative position of the uas.
- **Asynchronous observations** If ranging and GNSS observations are available asynchronously at different time instants, ranging observations can be incorporated in a separate update step using

$$\begin{aligned} y_k &= r(i,j)_k \\ &= ||d_{i,j,k}|| + \overline{w}_{r,k} \end{aligned} \tag{28}$$

$$C = \frac{\partial r}{\partial d}|_{d=\hat{x}_{k,k-1}} \tag{29}$$

It facilitates an informed judgment of the merits of the proposed set membership filter to compare it to the its stochastic EKF counterpart, to which we will turn our attention in the following section.

IV. Simulations and evaluation of the proposed strategy

To evaluate the proposed localization schemes, we consider two UAS in close proximity. Each UAS is assumed to broadcast its carrier phase and code phase observations as well as to take UWB range measurements. We select a half circle trajectory of relative positions of the follower UAS w.r.t. the predecessor, emulating a follower changing stations inside a formation, a maneuver requiring guaranteed but not overly conservative relative position estimation error bounds for safe but fast execution. Recall that for tight formation flight we want a filter that converges fast to useful, i.e. not overly conservative outer estimates of a set that is guaranteed to contain the relative position.
We consider three figures of merit to compare ESMF and EKF as well as to judge the impact of UWB ranging observations. First, the trace of the respective ellipsoid matrices (For the EKF we consider the 3σ level surface ellipsoid), as it gives a scalar measure of the ellipsoid size and thus its relative conservativeness. Second, the distance between the respective ellipsoid center and the relative position vector, representing the usefulness of the ellipsoid center as point state estimate. Third, plugging the true relative position into equation (Eq.1) provides a measure of distance to the ellipsoid surface indicating whether the guaranteed state set indeed contains the true state at all times.

GNSS observation errors When comparing the EKF, based on a normally distributed, i.e. unbounded process and measurement error model, and the ESMF and BPDMF, based on interval noise bounds, care has to be taken when it comes to simulating observation errors, as the assumed distribution inherently favors one or another filter formulation. While a simulated normal distribution obviously unduly favors the EKF, a uniform distribution is even further from realistic. From inspection of real zero baseline code phase double difference samples, it appears that the noise profile could reasonably be approximated by a biased normal distribution. However, even more realism can be introduced by directly using noise samples from zero-baseline experiments in simulation, thereby removing the need for assumptions about the statistical nature of double difference observation errors. This approach has been adopted here to simulate both differenced carrier phase as well as differenced code phase observations.
UWB ranging observation errors Our field experiments with a pair of UWB ranging devices (DecaWave $EVK1000$) indicate a range maximum error excluding antenna position offsets of $\overline{\omega}_r = 0.5m$ in unobstructed outdoor conditions. Larger error bounds reported in [10] are most likely due to the considered metal-rich industrial indoor environment that is not representative of the conditions expected within a formation of UAS made mostly of composite material. For simulation we draw observation errors from a uniform distribution.
Satellite constellation A static constellation of 7 satellites on a sphere corresponding to GPS orbits, constrained by a minimum elevation of 15% is simulated.
First, the GNSS observations are used. Fig. 1 shows how the ESMF guaranteed state ellipsoid fulfills its primary property and at all epochs contains the true relative position. The ellipsoid contracts drastically over the first few epochs to a quasi steady state in all three axes with a largest half axes of about 6 m.

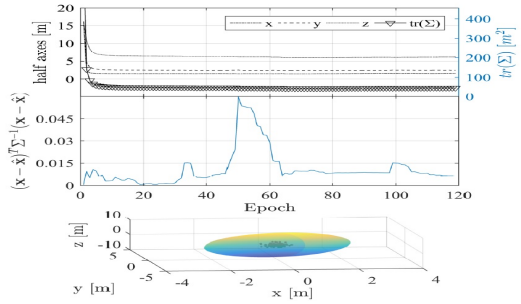

Fig. 1. ESMF, GNSS only: half axes of guaranteed state set, ellipsoid membership of true state, guaranteed state set at last epoch with pseudo range positions and ESMF position estimates

The EKF 3σ level set ellipsoid is by one order of magnitude more optimistic in Fig. 2 freeing up considerably more maneuvering space. The ellipsoid contains however from about epoch 45 on no longer the true relative position in Fig.3 illustrating the fundamental limitation of Kalman filtering for this application. Note that the EKF estimates an inconsistent

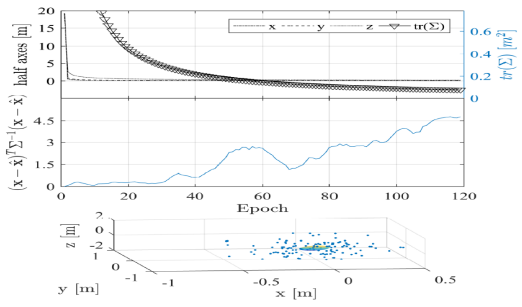

Fig. 2. EKF, GNSS only: half axes of ellipsoid $\Sigma_{3\sigma}$, ellipsoid membership of true state for $\Sigma_{3\sigma}$ at last epoch with pseudo range positions and KF position estimates

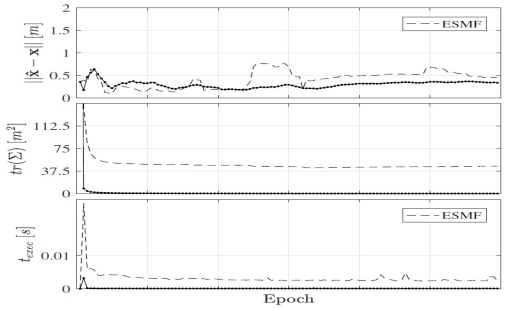

Fig. 3. GNSS only, comparison of ESMF, EKF: norm of center estimation error, size of guaranteed set (ESMF) or 3σ level set (EKF) respectively as measured by matrix trace, filter execution time

confidence ellipsoid in spite of differential pseudo range noise being well approximated by a zero mean normal distribution, i.e. although operating under rather favorable conditions. While both the EKF mean state estimate and the ESMF ellipsoid center approximate the true relative position with sub-meter accuracy, the EKF provides a smoother estimate. Note that fluctuations in filter execution times (an interpreted Matlab implementation running on a $4-corei7$ CPU on Windows 7 OS) can be attributed to the non-real-time execution environment.

Remark 3: Incorporating inter UAS range observations leads to tighter guaranteed state ellipsoids of the estimation in Fig. 4. The benefit of incorporating ranging observations

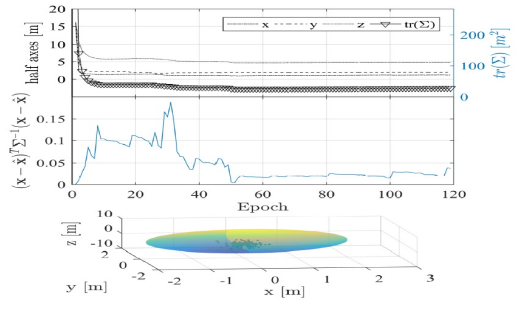

Fig. 4. ESMF, GNSS+UWB ranging

is more clearly illustrated by Fig. 5 displaying the ratio of the ESMF a posteriori half axes and trace without and with ranging observations. A reduction in size of by roughly 30% can be observed compared to the GNSS only case. As a

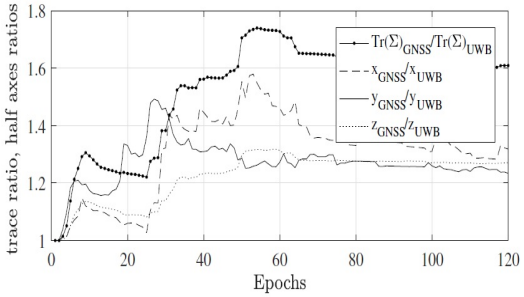

Fig. 5. ESMF: Ratios of ellipsoid volume and half axes with and without UWB ranging

first suggestion after these investigations, authors propose using the superior point estimation accuracy of the EKF for guidance purposes while relying on the confidence ellipsoid of the ESMF for guaranteed collision avoidance.

V. Conclusion

In this work, we have presented ellipsoidal sets that are guaranteed to contain the position of an UAS in a formation flight dispay. The relative positions of other UAS can be efficiently computed with a modified version of the Extended Set Membership Filter, relying on low-cost GNSS receiver and UWB ranging hardware. The performed simulations suggest that the resulting algorithm is suited for simultaneously tracking multiple UAS in real-time due to its moderate computational cost.

References

[1] M. Pachter, J. J. D'Azzo, and A. W. Proud, "Tight formation flight control," *Journal of Guidance, Control, and Dynamics*, vol. 24, no. 2, pp. 246–254, 2001.

[2] D. Borio, F. Dovis, H. Kuusniemi, and L. L. Presti, "Impact and detection of gnss jammers on consumer grade satellite navigation receivers," *Proceedings of the IEEE*, vol. 104, no. 6, pp. 1233–1245, 2016.

[3] R. M. Faheem, S. Aziz, A. Khalid, M. Bashir, and A. Yasin, "Uav emergency landing site selection system using machine vision," *Journal of Machine Intelligence*, vol. 1, no. 1, pp. 13–20, 2015.

[4] R. A. Garcia, G. V. Raffo, M. G. Ortega, and F. R. Rubio, "Guaranteed quadrotor position estimation based on gps refreshing measurements." *IFAC-PapersOnLine*, vol. 48, no. 9, pp. 67–72, 2015.

[5] E. Hansen and G. W. Walster, *Global optimization using interval analysis: revised and expanded*. CRC Press, 2003, vol. 264.

[6] S. B. Pope, "Algorithms for ellipsoids," *Cornell University Report No. FDA*, pp. 08–01, 2008.

[7] E. Scholte and M. E. Campbell, "A nonlinear set-membership filter for on-line applications," *International Journal of Robust and Nonlinear Control*, vol. 13, no. 15, pp. 1337–1358, 2003.

[8] C. Durieu, E. Walter, and B. Polyak, "Set-membership estimation with the trace criterion made simpler than with the determinant criterion," *IFAC Proceedings Volumes*, vol. 33, no. 15, pp. 1007–1012, 2000.

[9] D. Maksarov and J. Norton, "Computationally efficient algorithms for state estimation with ellipsoidal approximations," *International Journal of Adaptive Control and Signal Processing*, vol. 16, no. 6, pp. 411–434, 2002.

[10] A. R. J. Ruiz and F. S. Granja, "Comparing ubisense, bespoon, and decawave uwb location systems: Indoor performance analysis," *IEEE Transactions on Instrumentation and Measurement*, 2017.